Atomic Force Microscopy Study on Structure and Properties of Irradiation Grafted Silica Particles in Polypropylene-Based Nanocomposites

MING QIU ZHANG,[1,2] MIN ZHI RONG,[1] HAN MIN ZENG,[2] STEFAN SCHMITT,[3] BERND WETZEL,[3] KLAUS FRIEDRICH[3]

[1] Materials Science Institute, Zhongshan University, Guangzhou 510275, People's Republic of China

[2] Key Laboratory of Polymeric Composite and Functional Materials, The Ministry of Education of China, Zhongshan University, Guangzhou 510275, People's Republic of China

[3] Institute for Composite Materials (IVW), University of Kaiserslautern, D-67663 Kaiserslautern, Germany

Received 9 March 2000; accepted 2 August 2000

ABSTRACT: Nanosilica particles treated by irradiation grafting polymerization can effectively improve the strength and toughness of a thermoplastic polymer at a rather low filler content. A detailed investigation on the modified nanoparticles in the absence and presence of a polypropylene matrix is carried out by using atomic force microscopy. The results indicate that the loosen agglomerates of the untreated SiO_2 became more compact due to the linkage between the nanoparticles offered by the grafting polymer. In addition, the molecules of the polypropylene matrix are able to diffuse into the modified nanoparticle agglomerates during the melt processing. Entanglement between the molecules of the grafting polymer and the matrix is thus available, which in turn facilitates a strong particle–matrix interfacial interaction. © 2001 John Wiley & Sons, Inc. J Appl Polym Sci 80: 2218–2227, 2001

Key words: nanocomposites; nanoparticles; polypropylene; atomic force microscopy; force curve; nanoscale indentation tests

INTRODUCTION

The incorporation of nanoscale particles into a neat polymer matrix leads to a strong interfacial interaction when their ultrafine phase dimensions are maintained after compounding. In that case, nanocomposites possess a significant improvement in rigidity and reinforcement at a filler content far less than comparable glass or mineral reinforced polymers.[1]

However, polymer-based nanocomposites are very difficult to produce by the use of processing techniques common to conventional plastics. This is due to the strong tendency of the nanoparticles to agglomerate. Consequently, the so-called nanoparticle filled polymers sometimes contain a number of loosened clusters of particles and exhibit properties even worse than conventional particle–polymer systems. The following four approaches were developed[2–8] to break down nanoparticles

Correspondence to: M. Q. Zhang (ceszmq@zsulink.zsu.edu.cn).

Contract grant sponsor: Deutsche Forschungsgemeinschaft; contract grant number: DFG FR675/40-1.

Contract grant sponsor: National Natural Science Foundation of China; contract grant number: 59725307.

Contract grant sponsor: Team Project of the National Science Foundation of Guangdong.

Contract grant sponsor: Key Programs of the Ministry of Education of China; contract grant numbers: 98069, 99198.

Contract grant sponsor: Natural Science Foundation of Guangdong; contract grant number: 990277.

Journal of Applied Polymer Science, Vol. 80, 2218–2227 (2001)

agglomerates and to produce nanostructured composites: *in situ* polymerization of metal alkoxides in organic matrices via the sol–gel technique, intercalation polymerization by inserting polymer chains into sheets of smectite clay and other layered inorganic materials, the addition of organically modified nanoparticles to a polymer solution, and *in situ* polymerization of monomers in the presence of nanoparticles. Because the above techniques are characterized by complex polymerization procedures and special conditions and require polymerization equipment and solvent recovery, evidently a mass production of nanocomposites with cost effectiveness and applicability has to follow another route.

By examining the current technical level and the feasibility of the available processing methods, it can be concluded that the widely used compounding techniques for the preparation of conventionally filled polymers are still the most convenient ways when nanoparticles are proposed to replace micron-scale fillers for the purposes of performance enhancement without variation of the processability and density of the resultant composites. The problem is that nanoparticle agglomerates are also hard to disconnect by the limited shear force in polymer melts, which are characterized by high viscosity during melt mixing. This is true even when a coupling agent is used.[9] Because the latter can only react with the exterior nanoparticles, the agglomerates will maintain their friable structure in the composite and can provide neither reinforcing nor toughening effects.[10]

Based on the above analyses, our research emphasis was shifted from the attempts of pursuiting a nanoscale dispersion of the particles to the modification of the agglomerates themselves by means of an irradiation grafting treatment.[11] The results showed that the strength and toughness of thermoplastics can be significantly improved by the addition of only a small amount of modified nanoparticles (typically <3 vol %) using existing compounding techniques.[12,13] Such a simultaneous enhancement in tensile strength, modulus, and elongation at break (Fig. 1) is hard to find in conventional particulate composites. It is believed that a strong interfacial interaction due to the molecular entanglement of the grafting polymers and the matrix polymer rather than a strict miscibility matching between them accounts for the performance improvement. That is, much more species of monomers can be chosen for the grafting polymerization onto the nanoparticles, so that the mechanical properties of the nanocomposites

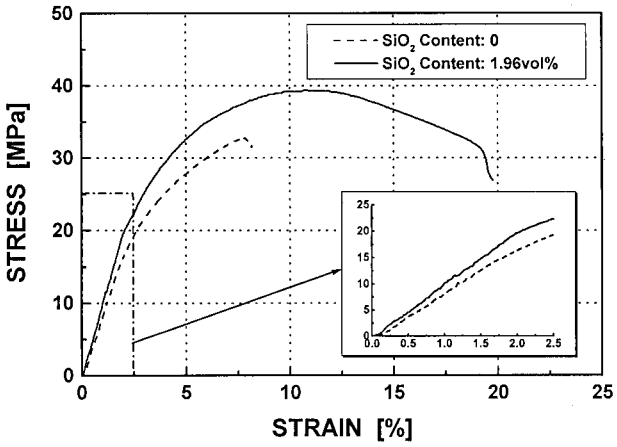

Figure 1 A typical tensile stress–strain curve of a SiO_2/polypropylene nanocomposite with polystyrene as the grafting polymer on the nano-SiO_2 in comparison to that of the unfilled polypropylene.

can be purposely adjusted according to the different interfacial viscoelastic properties introduced.

Although our previous studies revealed the effectiveness of the modified nanoparticles in strengthening and toughening of thermoplastics, microstructural details of the particles and the composites still lack thorough research, which limits a full understanding of the mechanisms involved. Because atomic force microscopy (AFM) is able to characterize the surface structure, morphology, and properties of materials from nanometer to millimeter scales, it is a suitable starting point to generate the related information about the irradiation grafted nanoparticles by means of this technique. Therefore, the objective of this study was to look into the fundamental aspects of the modified nanosilica (SiO_2) and its polypropylene (PP)-based composites by AFM, with particular interest in the structure and properties of the nanoparticle agglomerates in the presence of PP spherulites. In this way we hope to form a solid basis for further research on this new type of nanocomposite.

EXPERIMENTAL

The nanoparticles consisted of pyrogenic colloidal SiO_2 (Aerosol 1380, Degussa Co., Germany) with an average primary particle size of 7 nm and a specific gravity of 2.2 g/cm^3. Commercial styrene was used as the grafting monomer without further purification. The pregrafting of the nanoparticles by irradiation followed the procedures described in the literature.[12] Powdered isotactic PP

[Coathylene® PM050, melt flow index (MFI) = 120 g/10 min, 400-μm diameter, Herberts Polymer Powders] was used as the matrix polymer in this work. Granulated polystyrene (PS, type 143E, MFI = 10.5 g/10 min, BASF) was used as a reference when the force curves of different materials were measured by AFM.

To prepare the composite specimens for the AFM characterization, the untreated nano-SiO_2 and the PS grafted nano-SiO_2 (SiO_2-*g*-PS) were mixed thoroughly with the powdered PP at a SiO_2 loading of about 15 vol % using a mortar. The significantly higher filler content as compared with that required for the optimum mechanical performance of the nanocomposites[12,13] was chosen in order to facilitate a quick location of the regions of interest under the AFM microscope. The mixture of the nanoparticles and PP was heated to 210°C in a heating stage and kept at that temperature for 5 min, and then it was cooled to 134°C as quickly as possible allowing a crystallization of 120 min at this temperature. For a comparative study, neat PP was also crystallized under the same conditions.

Prior to the AFM observation, the PP and its composite specimens were both etched using a permanganic etchant[14] in order to expose the microstructures to the AFM microscope probe tip.

A commercial AFM microscope (Nanoscope III, Digital Instruments) was used. All the measurements were conducted in air. The specimen to be tested was placed on a piezoelectric tube scanner that enables an accurate scan in the horizontal (x–y) plane while moving in the vertical (z) direction (Fig. 2). The tapping mode was used in the imaging of the surface morphologies of the specimens. In addition, nanoscale indentation tests were also carried out using the tapping mode tip under the framework of lithography driven by the NanoScript™ language. The tip deflection voltage was set to 5 V, which led to an indentation depth of about 65 nm. The probe spring constant was 38 N/m.

To measure the elasticity of the specimens, the contact mode was executed by recording the force curves. Typically these curves show the deflection of the free end of the cantilever as the fixed end of the cantilever is brought vertically toward and then away from the sample surface.

It should be emphasized that during the above nanoindentation and force plots measurements of different specimens, the tapping mode and the contact mode tips were not changed, so the related operation parameters were maintained constant. This allowed a direct comparison between the results.

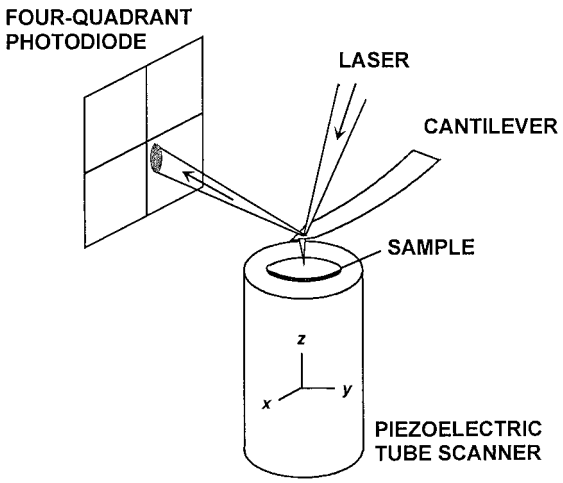

Figure 2 A schematic diagram of the AFM setup. Cantilever movements are measured by the reflected laser beam with a four-quadrant photodiode.

RESULTS AND DISCUSSION

AFM Characterization of Nanoparticles

The morphologies of nano-SiO_2 agglomerates before and after grafting are shown in Figure 3. (The images are height ones, which are the same as the rest of the AFM images in this article.) Note that the latter has a rougher appearance, implying that the particle modification has resulted in finer aggregates. (It should be declared here that, when dealing with the microstructure of the nanoparticles, the following terms are used in this article in the order of their size: primary particles < aggregates < agglomerates < clusters, where the aggregates are the smallest detectable unit under the current condition.) This is factually a reflection of the grafting polymerization on the nanoparticles. Because of the low molecular weight nature, the grafting monomers can penetrate into the agglomerated nanoparticles easily and react with the activated sites of the nanoparticles inside and outside the agglomerates. In this way, the originally loosened clusters of particles were transformed into a nanocomposite microstructure comprising the nanoparticles and the grafted, homopolymerized PS, which was proved by the spectral analyses.[12,13]

Obviously, Figure 3 indicates that the SiO_2-*g*-PS possesses a higher specific surface area than SiO_2 as received. Like other porous particles, this

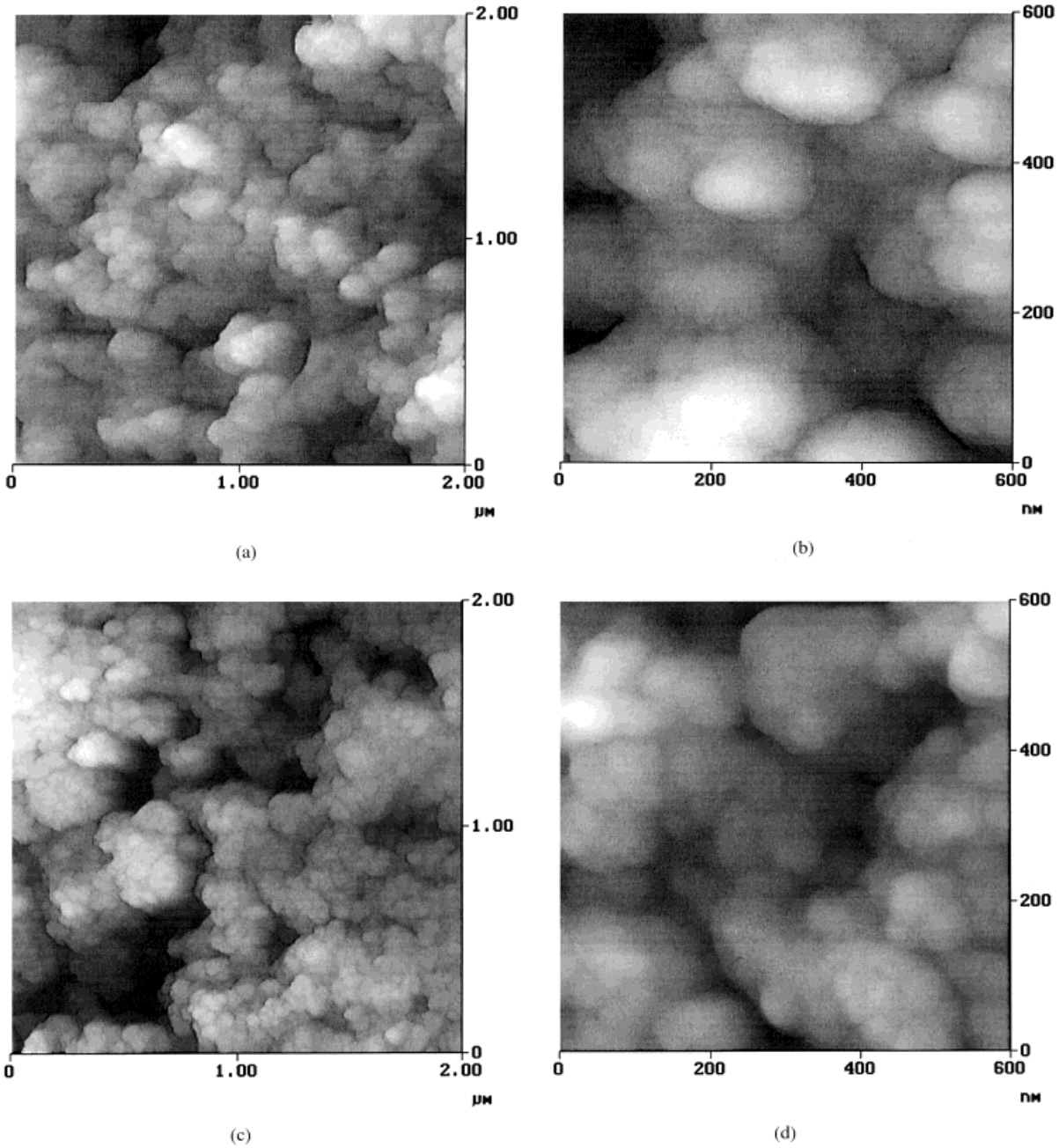

Figure 3 AFM images of (a,b) nano-SiO_2 as received and (c,d) SiO_2-*g*-PS.

leads to a higher volume fraction per unit weight of the former in a polymer matrix. It can, in turn, partially explain that the untreated nano-SiO_2 particles are less effective in improving the mechanical properties of the thermoplastic matrix in comparison to the SiO_2-*g*-PS aggregates under the same SiO_2 content, because the reinforcing and toughening effects are usually related to the volumetric effect of the fillers. Besides, the higher specific area of SiO_2-*g*-PS will also facilitate the absorption of more matrix molecules with lower molecular weight in the composites so that the interfacial interactions are enhanced.

In addition, it can be expected that the modified nanoparticle agglomerates possessing some molecular links inside of them (due to the grafting procedure) become stronger. This is true as illustrated by the tip deflection curves given in Figure 4. For a better understanding of the testing principle and the meaning of these curves, Figure 5 gives a stepwise description of the measurement. In step 1 the cantilever is far away from the

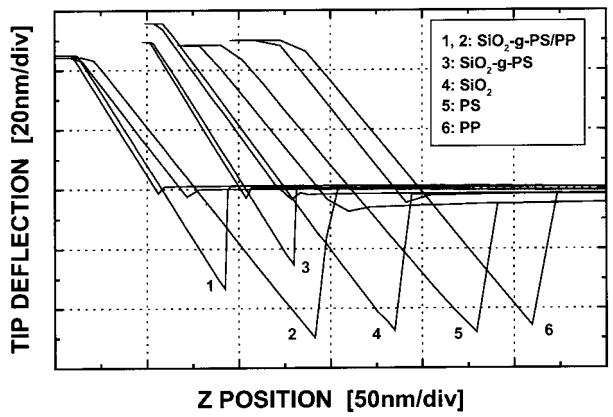

Figure 4 A typical cantilever deflection versus z scan of different materials.

specimen and no deflection occurs. As the cantilever is brought closer to the specimen in step 2, the tip senses the attractive force from the specimen, which causes the free end of the cantilever to bend downward or to jump into contact with the specimen in case the attractive force gradient exceeds the spring constant of the cantilever. In step 3 the cantilever deflection continues to increase in the other direction as the fixed end of the cantilever is brought much closer to the specimen. The corresponding slope of the plot can provide information about the elasticity of the specimen surface. Then the motion is reversed in step 4. The adhesion between the tip and the specimen maintains the contact, although there is now a tensile load. The tensile load overcomes the adhesion and the tip snaps out of contact with the specimen in step 5. This can be used to measure the rupture force required to break the adhesion. Returning to the force plots of the nano-SiO_2 in Figure 4, the slope of the repulsive portion of the curve for the untreated nano-SiO_2 (curve 4) is found to be smaller than that for the SiO_2-*g*-PS (curve 3). Because a softer material would result in less deflection of the cantilever under a given displacement in the vertical direction, the result actually demonstrates that SiO_2-*g*-PS has higher stiffness. Considering that the total displacement during the tip, when being pressed into the specimen surface, is about 50 nm or larger (Fig. 4), which is much larger than the size of a primary SiO_2 particle (~7 nm), the above-mentioned difference in elasticity between SiO_2 as received and SiO_2-*g*-PS should manifest the difference in the bulk elasticity of the nanoparticle agglomerates. In other words, the lower stiffness of the agglomerated SiO_2 determined from the slope of curve 4 in Figure 4 is not merely an intrinsic material property of SiO_2 ($\text{modulus}_{\text{silica}}$ = 70 GPa) but also includes the contribution of interparticle nanoscale displacement in response to the force applied by the cantilever. In contrast, the interparticle displacement in the SiO_2-*g*-PS agglomerates is hindered because the grafting polymer has combined the nanoparticles into a microcomposite structure.

AFM Characterization of Nanoparticles in PP-Based Composites

Figure 6 gives AFM micrographs of the spherulitic structure of the neat PP. Compared to traditional light microscopy, AFM is known for its ability to reveal delicate morphological details of a crystalline polymer. The crystalline structure of PP was previously studied with this technique.[15–17] Because the target of the present study was not a morphological characterization of PP, the details of Figure 6 are not discussed.

It is interesting to see the spherulitic structure was not influenced by the incorporation of the nanoparticles (Fig. 7). In addition, there was no significant evidence showing that larger agglomerates of the untreated SiO_2 acted as the nucleation sites of the PP spherulites. The typical sizes of the SiO_2 agglomerates in the PP matrix determined from Figure 7 were around 100–300 nm, much smaller than those of the SiO_2-*g*-PS (Fig. 8). These coincided with the results of an isothermal crystallization investigation of the same materials with differential scanning calorimetry (DSC) cells.[12] The thermal analyses indicated that the crystalline characteristics of the PP matrix had not changed under the presence of both untreated and modified SiO_2, and the untreated SiO_2 had a more profound nucleation effect on PP than the grafted version. Based on the AFM images ob-

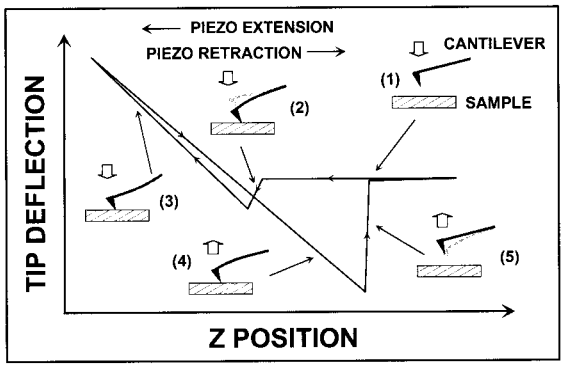

Figure 5 A schematic drawing displaying the cantilever bending as a function of the sample displacement.

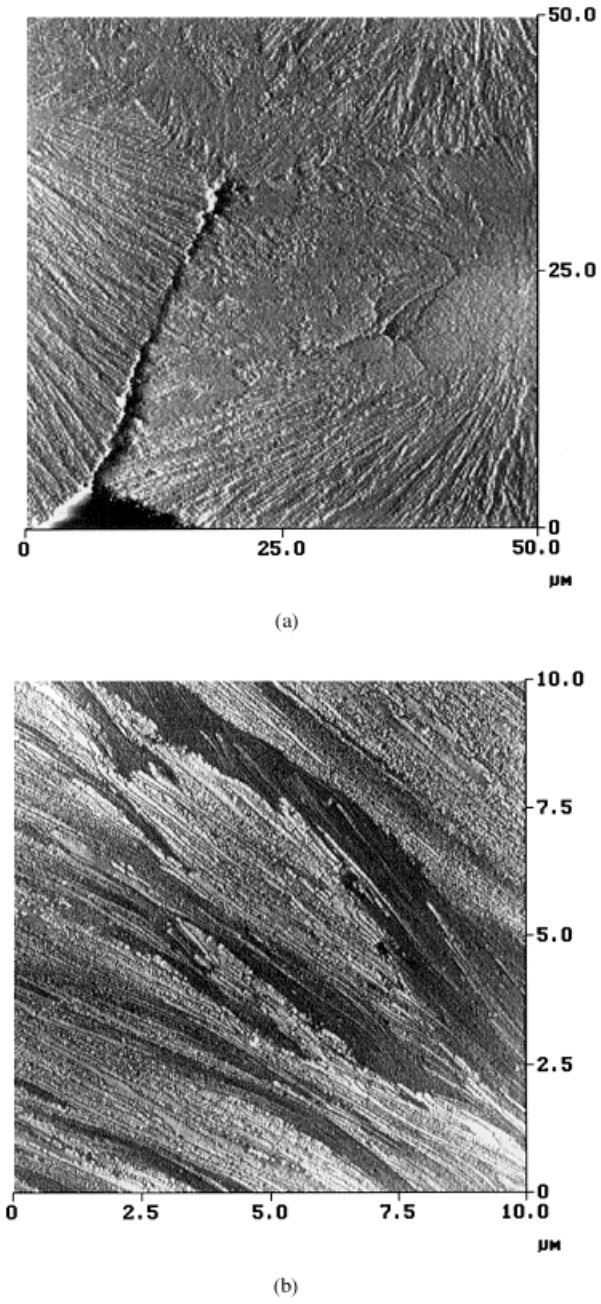

Figure 6 AFM images of etched PP: (a) spherulites and (b) a close-up of the lamellae structure.

tained here, it can be deduced that the higher crystallization rate of the untreated SiO_2/PP system originated from the fact that the as-received SiO_2 particles were dispersed in the matrix in the form of tiny agglomerates, which facilitated more particle–matrix contacts.

With respect to the distribution characteristics of the nanoparticles, it can be found from Figure 7 that they were either located at the fanlike radiated lamellae [Fig. 7(b)] or pushed to the spherulites boundaries [Fig. 7(c)], besides those serving as the heterogeneous nuclei. It was also evident that in general that there was no strong interfacial interaction between the particles and the matrix. Therefore, it can be expected that this led to rather low mechanical properties of the composites because of the breaking and splitting of the agglomerated nanoparticles.

In the case of SiO_2-*g*-PS/PP (Fig. 8), however, the images were quite different. The agglomerates were much larger than those of the untreated SiO_2 (Fig. 7) and a chainlike branched structure of the agglomerated SiO_2-*g*-PS was seen [Fig. 8(c)]. Note that the size of the particle agglomerates was different than the size observed by transmission electron microscopy (TEM).[12] This must have been a result of differences in the preparation procedure of the samples. (The components were mixed by a single screw extruder in Rong et al.[12]) The larger clusters of the untreated SiO_2 found in the PP matrix by TEM actually indicated that the nanoparticle agglomerates were more difficult to disconnect in the polymer melt during compounding compared to the modified nanoparticles. It can be considered that the present AFM imaging produced a more exact revelation of the basic morphologies of the nanoparticles in the PP matrix, because here more realistic nanocomposites were investigated (even when still on a model type level).

The distinct chainlike appearance of the SiO_2-*g*-PS agglomerates in the PP further demonstrated the role of the grafting polymer (i.e. separating) but still connected the nanoparticles. Unlike the untreated SiO_2, the nanoparticles in the SiO_2-*g*-PS agglomerates bound to the grafting PS coupled with a certain viscoelasticity. Therefore, a percolation of the shear yielded regions inside such agglomerates became possible, which was assumed to be one of the toughening mechanisms involved in the nanocomposites.[12] Besides, the chainlike branched agglomerates of SiO_2-*g*-PS might provide the matrix with better loading ability because they have significantly higher aspect ratios than the individual particles.

Although the SiO_2-*g*-PS agglomerates di not have strong nucleation effects on the PP, as reflected by Figure 8(c) and the DSC measurements,[12] this does not mean that there was no interaction between the particles and the matrix. Figure 8(d) shows a cave left by the etching process. Obviously some nanoparticle agglomerates had been there and were removed later by the etchant because of the higher rate of etching of the amorphous PS. However, the nanoparticles

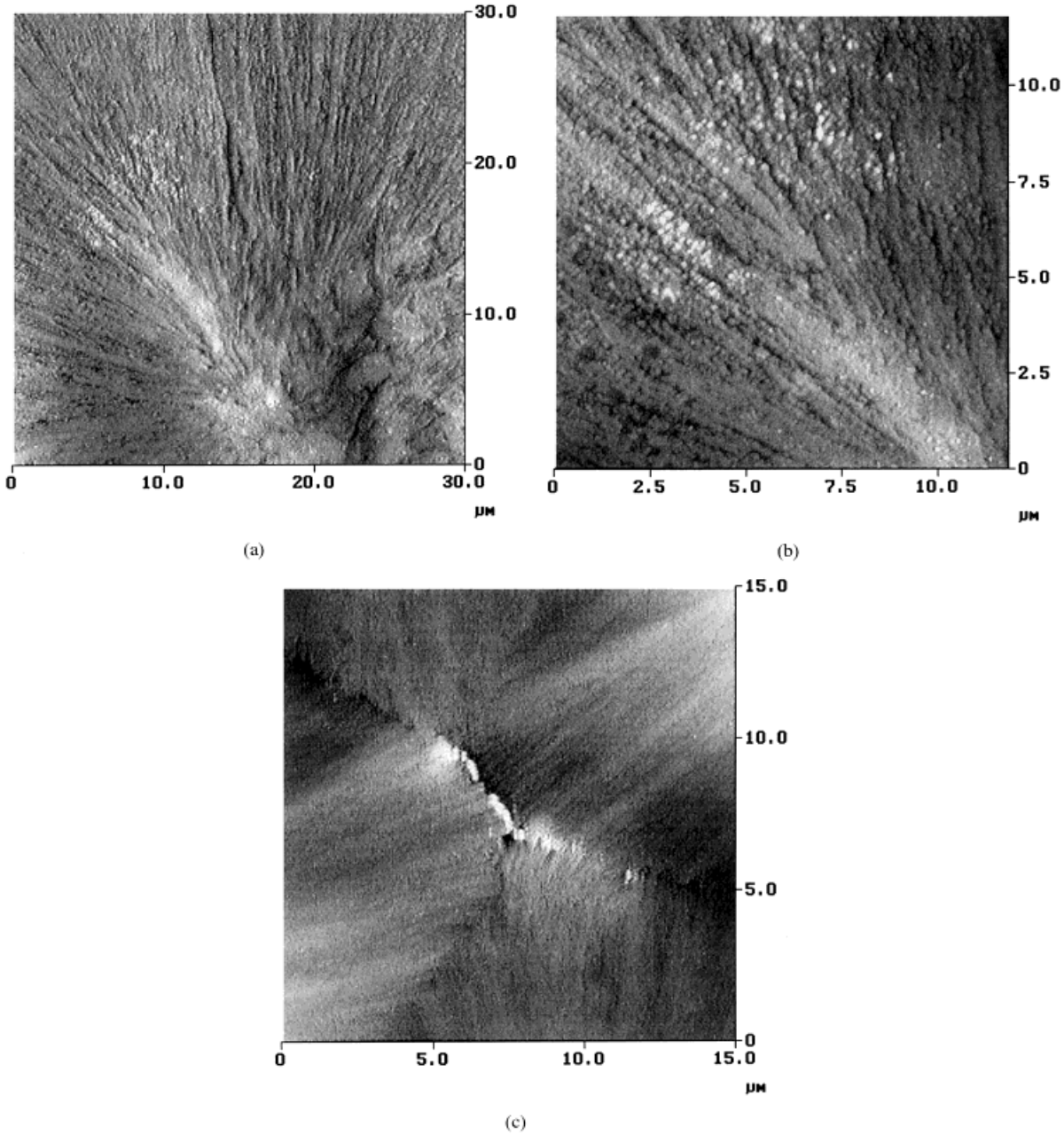

Figure 7 AFM images of etched nano-SiO_2/PP: (a) a spherulite of PP with its center near the bottom of the micrograph, (b) a magnified image of that spherulite, and (c) the boundaries of the spherulites.

clusters that remained at the edge of the cave prove the above-mentioned statement. The PP lamellae must have fully penetrated them to hold them in place, and also the PP lamellae penetrating the cave (arrow) demonstrate that molecules of the PP melt were able to immigrate into the nanoparticle agglomerates. An interdiffusion and entanglement between the molecules of the grafting polymers and the matrix can thus take place outside and inside the nanoparticle agglomerates. Because the present specimens were prepared in a hot stage without further shear mixing when the heating started, it can be concluded that the above observation should also conform to the nanocomposites prepared by melt compounding in an extruder.[12]

Figure 4 also exhibits the force curves of PP, PS, and SiO_2-*g*-PS in the PP matrix. Contrary to the other materials, a rather long-range attraction, which caused the cantilever to deflect down-

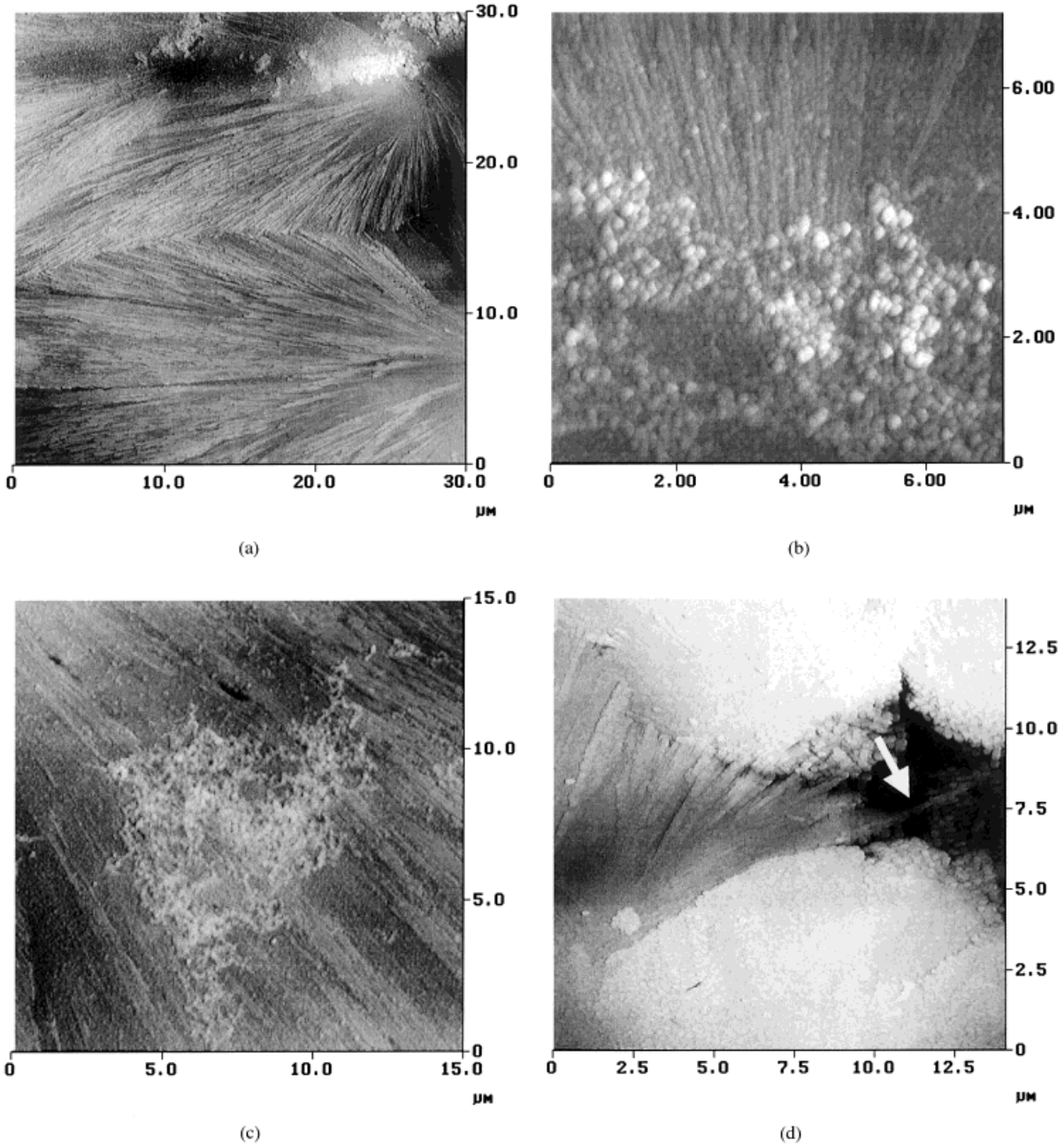

Figure 8 AFM images of etched SiO_2-*g*-PS/PP: (a) spherulites of PP in which the nanoparticles act as nucleation sites at the right upper corner of the figure, (b) radiated lamellae nucleated by the nanoparticles, (c) agglomerated SiO_2-*g*-PS dispersed in the lamellae, and (d) PP lamellae penetrating the cave resulting from etching of the SiO_2-*g*-PS agglomerates.

ward before it contacted the sample surface, can be seen from the plot of PS. This could be a result of its molecular characteristics. But because the specimens in air might be covered by a thin layer of water or other contaminants (which interfere with the AFM imaging[18]), a discussion on the surface properties of the specimens is not be made under the present experimental conditions.

Nevertheless, it is still possible to compare the elasticity of the materials by using the force curves shown in Figure 4. It is clear that the PP and PS had similar elasticity, which was the lowest among the specimens tested, suggesting the present AFM tip with particular cantilever spring constant was not sensitive enough to distinguish such differences in the modulus. Curves 1 and 2

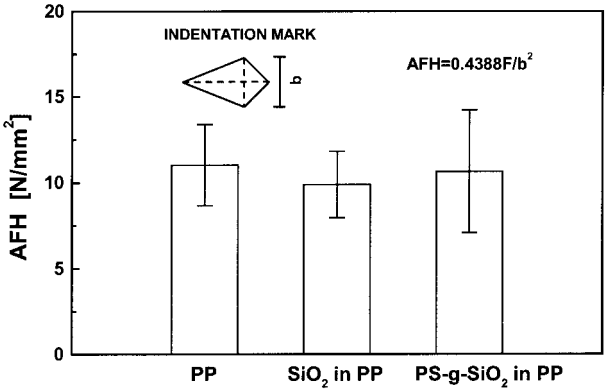

Figure 9 The microhardness of PP and the nanoparticles in the PP matrix.

were measured on SiO_2-*g*-PS agglomerated SiO_2-*g*-PS dispersed in the PP matrix. Here the effect of a long-range attraction of the PS was no longer visible (curves 1–3), which was probably due to less of a fraction and the lower molecular weight of the grafting PS.[12] In addition, it was interesting to find that curves 1 and 2 were quite different. The slope of the repulsive portion of curve 1 is similar to that of the particles tested alone (curve 3), while the slope of curve 2 is similar to that of the matrix tested alone (curve 6). Because it was impossible to "see" the exact point on which the force curve was being measured, for the moment we cannot confirm that the above difference results from either the difference between the nanoparticles-rich phase and the matrix-rich phase or the differences between the nanoparticles containing the penetrating PP molecules and the particles maintaining their original structure. Further study is needed to clarify this.

The microhardness values of the untreated and treated SiO_2 in PP, as well as the PP matrix, are given in Figure 9. The corresponding nanoscale indentations were conducted on the particles and the matrix of the same sample [Fig. 10(a)]. The hardness determined by AFM (AFH) was calculated from the minor axis of the rhombic indentation marks (b) as follows[19]:

$$\mathrm{AFH} = 0.4388\,\frac{F}{b^2} \qquad (1)$$

where F denotes the force applied. The data of Figure 9 suggest that under the present testing conditions the nanoparticle agglomerates of SiO_2 in the PP matrix offer little in the way of hardness. This implies that on the nanoscale the agglomerates cannot be taken as the fillers that are much harder than the matrix polymer. In other words, they play only the role of physically and/or chemically crosslinking sites in the matrix. From Figure 10(b) it can be seen that the concave indentation mark partially "healed" due to the elastic recovery of the pile-ups at the edges. As the AFM probe tip was brought into contact with the agglomerated SiO_2-*g*-PS during the indentation test, the micrograph of Figure 10(b) actually indicates that the raised material at the indentation edges must consist of both the modified nanoparticles and the matrix polymer. It is the latter that provides the "self-healing" ability for the indentation mark. Considering that the indentation depth (~65 nm) is larger than the size of the

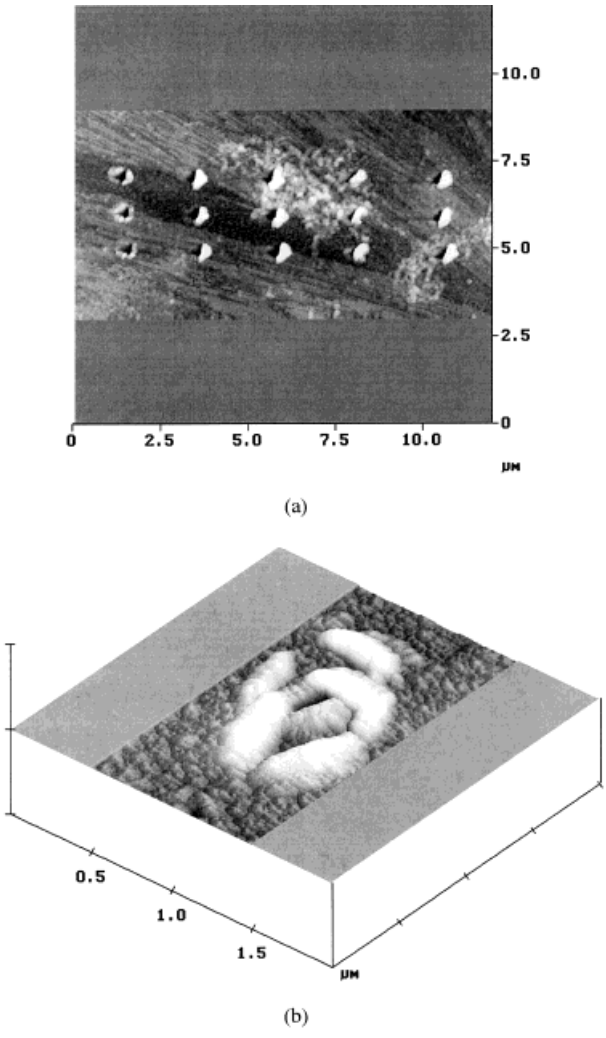

Figure 10 (a) A typical AFM image of the nanoindentation marks on etched SiO_2-*g*-PS/PP. (b) A magnified AFM surface plot of an indentation mark on an agglomerated SiO_2-*g*-PS in the PP matrix. One division in the vertical axis corresponds to 450 nm. Both were scanned after the indentation tests.

primary particles (~7 nm) but smaller than that of the agglomerated particles, it can be further evidenced that the matrix PP has diffused into the agglomerates. This is in agreement with the analyses of Figure 8(d) and the estimation made in the literature.[12,13]

CONCLUSIONS

Based on the above AFM investigations, the following statements can be made.

1. AFM is an effective tool to characterize nanocomposites by providing the morphological, mechanical, and physical information.
2. The nano-SiO_2 particles modified through the irradiation grafting polymerization had reduced aggregate size and higher specific surface area, as well as a more compact agglomeration structure. This, in turn, improved the mechanical properties of the polymer matrix more effectively than the untreated nanoparticles.
3. The SiO_2 nanoparticles in the as-received form, as well as SiO_2-*g*-PS nanoparticles, did not exert a detectable influence on the crystalline structure of the PP matrix. During the melt crystallization process of PP, their agglomerates can partly serve as heterogeneous nuclei, but more probably they are dispersed among the lamellae or pushed to the spherulite boundaries.
4. The morphology of SiO_2-*g*-PS in the PP matrix was characterized by a chainlike branched structure. The SiO_2-*g*-PS agglomerates were stiffer but not harder than PP.
5. When PP was in a molten state, its molecules were able to immigrate into the agglomerated SiO_2-*g*-PS. As a result, entanglement between the molecules of the grafting polymer and the matrix inside and outside the agglomerates occurred.
6. The SiO_2-*g*-PS agglomerates in PP possessed a nanocomposite microstructure consisting of the nanoparticles, the grafted and homopolymerized PS, and the PP matrix.

Our financial support is gratefully acknowledged. Professor K. Friedrich is grateful to the Fonds der Chemischen Industrie, Frankfurt, for support of his personal research activities in the year 2000.

REFERENCES

1. Roy, R. Mater Sci Res 1986, 21, 25.
2. Novak, B. M. Adv Mater 1993, 5, 422.
3. Kojima, Y.; Usuki, A.; Kawasumi, M.; Okada, A.; Fukushima, Y.; Kurauchi, T.; Kamigaito, O. J Polym Sci Part A Polym Chem 1993, 31, 1755.
4. Yano, K.; Usuki, A.; Okada, A.; Kurauchi, T.; Kamigato, O. J Polym Sci Part A Polym Chem 1993, 31, 2493.
5. Giannelis, E. P. Adv Mater 1996, 8, 29.
6. Zilg, C.; Thomann, R.; Muelhaupt, R.; Finter, J. Adv Mater 1999, 11, 49.
7. Carrotenuto, G.; Nicolais, L.; Kuang, X.; Zhu, Z. Appl Compos Mater 1995, 2, 385.
8. Gonsalves, K. E.; Carlson, G.; Chen, X.; Gayen, S. K.; Perez, R.; Jose-Yacaman, M. Polym Mater Sci Eng 1995, 73, 298.
9. Xu, W.; Huang, R.; Cai, B.; Fan, W. Chin Plast 1998, 12, 30 [in Chinese].
10. Sumita, M.; Tsukumo, Y.; Miyasaka, K.; Ishikawa, K. J Mater Sci 1983, 18, 1758.
11. Rong, M. Z.; Zhang, M. Q.; Zheng, Y. X.; Zeng, H. M. Chin. Pat. Applic. CN99116017, 1999.
12. Rong, M. Z.; Zhang, M. Q.; Zheng, Y. X.; Zeng, H. M.; Walter, R.; Friedrich, K. Polymer 2001, 42, 167.
13. Zheng, Y. M.S. Thesis, Zhongshan University, 1999.
14. Olley, R. H.; Bassett, D. C. Polymer 1982, 23, 1707.
15. Vancso, G. J. In Polypropylene: An A–Z Reference; Karger-Kocsis, J., Ed.; Dordrecht: Kluwer, 1999; p 511.
16. Vancso, G. J.; Liu, G.; Karger-Kocsis, J.; Varga, J. Colloid Polym Sci 1997, 275, 181.
17. Wu, C.-M.; Chen, M.; Karger-Kocsis, J. Polym Bull 1998, 41, 239.
18. Weisenhorn, A. L.; Hansma, P. K.; Albrecht, T. R.; Quatt, C. F. Appl Phys Lett 1989, 54, 2651.
19. Weber, T. Anwendung der Rasterkraftmikroskopie und der Ultramikrohaerte zur Charakterisierung des Verhaltens ungefuellter Polymere unter kleinsten Lasten. IVW Research Report; Institute for Composite Materials: University of Kaiserslautern, Germany, 1998.